(8) Lantman, C. W.; MacKnight, W. J.; Higgins, J. S.; Peiffer, D. G.; Sinha, S. K.; Lundberg, R. D. *Macromolecules* **1988**, *21*, 1339.
(9) Hara, M.; Wu, J.; Jermone, R.; Granville, M. *Macromolecules* **1988**, *21*, 3331.
(10) Hara, M.; Wu, J. *Macromolecules* **1988**, *21*, 402 and references therein.
(11) Pedley, A. M.; Higgins, J. S.; Peiffer, D. G.; Burchard, W. Submitted for publication in *Macromolecules*.
(12) Elias, H. G. In *Light Scattering From Polymer Solutions*; Huglin, M. B., Ed.; Academic Press: New York, 1972.
(13) Lundberg, R. D.; Makowski, H. S. *J. Polym. Sci., Polym. Phys. Ed.* **1980**, *18*, 1821.
(14) Makowski, H. S.; Lundberg, R. D.; Westerman, L.; Bock, J. J. *Polym. Prepr. (Am. Chem. Soc., Div. Polym. Chem.)* **1978**, *19*, 292.
(15) Ullman, R. *J. Polym. Sci., Polym. Phys. Ed.* **1985**, *23*, 1477.
(16) Debye, P. *J. Phys. Colloid Chem.* **1947**, *51*, 18.
(17) King, J. S.; Boyer, W.; Wignal, G. D.; Ullman, R. *Macromolecules* **1985**, *8*, 709.
(18) Witten, T. A.; Schafer, L. *J. Chem. Phys.* **1981**, *74*, 2582.
(19) Ohta, T.; Oono, Y.; Freed, K. F. *Phys. Rev.* **1982**, *A25*, 2801.
(20) See, for example: Atkins, P. *Physical Chemistry*, 2nd ed.; Oxford University Press: Oxford, England, 1982.
(21) Forsman, W. C. pp 39–50 in ref 1.
(22) Witten, T. A. Lecture presented at International Symposium on Electrical Interactions in Complex Fluids Colmar; France, June 1987.
(23) Schulz, G. V.; Lechner, M. In *Light Scattering From Polymer Solutions*; Huglin M. B., Ed.; Academic: New York, 1972.
(24) Bandrup, Ed. *Polymer Handbook*; Wiley: New York, 1985.
(25) Kirkwood, J. G.; Riseman, J. *J. Chem. Phys.* **1948**, *16*, 565.
(26) Kirkwood, J. G.; Zwanzig, R. W.; Plock, R. J. *J. Chem. Phys.* **1955**, *23*, 213.
(27) Flory, P. J. *Principles of Polymer Chemistry*; Cornell University Press: Ithaca, NY 1953; Chapters x, xii, xiv.

Registry No. Neutron, 12586-31-1.

Static Light Scattering of Polyelectrolyte–Micelle Complexes

Paul L. Dubin,* Stephens S. Thé,† Leong Ming Gan,‡ and Chwee Har Chew‡

Department of Chemistry, Indiana University–Purdue University at Indianapolis, Indianapolis, Indiana 46205-2820. *Received August 14, 1989; Revised Manuscript Received December 7, 1989*

ABSTRACT: Soluble complexes are formed between poly(dimethyldiallylammonium chloride) and anionic/nonionic mixed micelles of sodium dodecyl sulfate and Triton X-100, at certain well-defined micelle compositions and ionic strengths. Static light scattering has been used to characterize the complexes generated from a 2×10^5 MW sample of this polycation and mixed micelles with 0.35 mol fraction anionic surfactant, at an ionic strength of 0.40 M. Measurements were carried out for polyion–micelle complexes at polymer concentrations ranging from 0.0025 g L^{-1} to 0.8 g L^{-1}, for surfactant-free polymer solutions, and for polymer-free micelle solutions. In the low polymer concentration range (<ca. 0.1 g L^{-1}) the results are consistent with intrapolyion complexes, with dimensions comparable to those of the free polymer, in which 10–20 micelles are bound. At higher polymer concentrations, higher order aggregates form. For a polymer sample with nominal MW of 2×10^6, such higher order aggregates appear to be present even at very low concentrations. The results suggest an equilibrium between intrapolymer and multipolymer complexes, that depends, inter alia, on polymer–micelle stoichiometry and on polymer chain length.

Introduction

Polymer–surfactant complexes have proved to be of enduring interest,[1–10] largely because the self-organization of macromolecules and low molecular weight amphiphiles into higher order structures offers some intriguing similarities to biological assemblies. For ionic surfactants above the critical micelle concentration (cmc) in the presence of oppositely charged polyelectrolytes, complex formation results from the Coulombic interaction of the polyion and the charged micelle.[11–18] Usually the interaction is very strong and a highly ion-paired amorphous precipitate forms at once. Attenuation of the interaction by reduction of the micelle surface charge density or by increase in ionic strength can totally suppress complex formation or, at intermediate micelle surface charge density or ionic strength, may lead to coacervation (liquid–liquid phase separation) in place of precipitation.[12,13] In one particular system, comprised of mixed anionic/nonionic micelles of SDS and Triton X-100, along with the strong polycation, poly(dimethyldiallylammonium chloride) (PDMDAAC), soluble complexes are formed over a reasonably wide range of conditions.[12,14,16]

We have studied these soluble complexes of SDS/TX-100/PDMDAAC by turbidimetry,[11–16] viscometry,[11] dynamic light scattering (QELS),[12,14,16] ultrafiltration,[16] and dye solubilization.[19] At an ionic strength of $I = 0.40$ M, such complexes are formed when the mole fraction of SDS in the mixed micelle, Y, is between 0.23 and 0.45. At $Y < 0.23$ the reduced specific viscosity of the mixture is the same as that of the surfactant-free solution, while the turbidity and the mean apparent diffusion coefficient by QELS are both equal to that of the polymer-free solution. From these findings, we may conclude that interactions at $Y < 0.23$ are too transient to detect by these methods. At $Y > 0.45$, i.e. at higher micelle surface charge densities, bulk phase separation takes place. At intermediate values of Y, complexation is reversible. Under such conditions, the mean apparent diffusion coefficient obtained by cumulants analysis[20] of the QELS autocorrelation function suggests that the hydrodynamic radius

† Current address: E. I. du Pont de Nemours & Co., Wilmington, DE 19880.
‡ Permanent address: Department of Chemistry, National University of Singapore, Singapore.

0024-9297/90/2223-2500$02.50/0

of the complex is ca. 20–40 nm; comparable values for PDMDAAC and the mixed micelle, under similar conditions, are 17 and 8 nm, respectively. More detailed QELS data, using various procedures to fit the autocorrelation curve to appropriate size distributions, reveal an equilibrium between the complex and unbound micelles, which may be perturbed by removing the micelles by ultrafiltration.[16]

The foregoing studies, in conjunction with the observation that critical conditions for complex formation are independent of the concentration of either polymer or total surfactant, led us to postulate the existence of an "intrapolyion" complex, in which one polymer binds some number of micelles. However, interpretation of the QELS results poses a number of problems. (1) Deconvolution of the autocorrelation function into multiple decays is a delicate process, and for bimodal systems, such as these mixtures of complex and unbound micelles, the two decay constants cannot be obtained with great precision. (2) In such macroionic systems, the possibility of long-range interactions among the scatterers, including coupled polyion–small-ion diffusions, must be considered; such interactions contribute to the apparent diffusivity and, if neglected, could lead to unrealistic apparent Stokes' radii. Therefore, in the present work, we sought to enhance our understanding of the structure of the complex by static light scattering. To establish conditions under which meaningful evaluations of the molecular mass of the complex could be made, we carried out a number of turbidimetric and dynamic light scattering measurements, as well.

Experimental Section

Materials. Poly(dimethyldiallylammonium chloride) (PDMDAAC) samples from Calgon Corp. (Pittsburgh, PA) were dialyzed and lyophilized. The nominal MWs of the two samples, commercial names "Merquat 100" and "Cat-floc", are 2×10^5 and 2×10^6, respectively. Size-exclusion chromatograms, reported elsewhere,[21] show that the distributions are extremely broad, with $\bar{M}_w/\bar{M}_n > 10$. Detailed SEC analysis[22] coupled with light scattering, shows very small $\bar{M}_n$ for Merquat 100, so that the polydispersity of the sample is largely a consequence of high oligomer concentration, as opposed to the presence of very high MW components. Sodium dodecyl sulfate (SDS) was Fluka (Happague, NY) "purissima" grade. Triton X-100 (TX-100) was from Rohm and Haas (Philadelphia, PA).

Methods. Turbidity measurements were made at 420 nm with a Brinkmann PC800 probe colorimeter, equipped with a 2.0-cm path length fiber optics probe. "Type 3" turbidimetric titrations[16] were carried out by the addition of PDMDAAC to a solution of SDS/TX-100 at constant ionic strength, at 23 ± 1 °C. The measured value of 100% T (which is essentially linear with the turbidity for % $T > 90$) was corrected by subtraction from turbidimetric titrations of a polymer-free blank.

QELS measurements were made at 90° scattering angle with a Malvern RR102 spectrometer, using a Jodon 20-mW HeNe laser as a light source. The spectrometer cell was maintained at 25.0 ± 0.1 °C in a toluene refractive index matching bath. The photomultiplier aperture was set between 0.5 and 2.0 mm. Data were collected and analyzed with a 64 channel Nicomp TC-100D autocorrelator/6800 computer or an Epson Equity II+ computer interfaced to the Nicomp TC-100D through Procomm version 2.3 communication software. Autocorrelation decay curves were interpreted by cumulants analysis[20] or by a more detailed deconvolution similar to the algorithms described by Provencher.[23] We have previously shown[14] that the bimodal size distributions for these polyion–micelle systems obtained this way are nearly identical with those found by using the nonnegative constrained least-squares method of Morrison and Grabowski.[24] Photon counts were acquired until the "fit error" and "residual"[25] were less than 2 and 5, respectively.

Static light scattering intensity measurements were made by using a 436-nm source, at scattering angles from 20° to 135°, with a Brice-Phoenix 2000D photogoniometer, modified to provide adequate air cooling so as to keep the temperature in the cell compartment between 23 and 25 °C. The sample cell was either a semioctagonal 40 × 40 mm cell or a small cylindrical cell (C.N. Wood). Photomultiplier response was measured after 5 min and repeated until two consistent readings were obtained. All solutions were repeatedly filtered through 0.2-μm porosity nylon filters (National Scientific) into scintillation vials, in a dust-free chamber, until no particulate matter could be observed in the HeNe laser beam.

PDMDAAC samples were prepared by dilution of stock solution with 0.40 M NaCl that had been previously dialyzed against the polymer. TX-100 solutions were diluted with 0.40 M NaCl + 0.2 g L^{-1} TX-100 (corresponding to the cmc). Mixed micelle solutions of SDS/TX-100 were prepared by dilution of C_S = 14 g L^{-1} stock solutions at the desired Y and I. Since the cmc of the mixed micelle is <0.1 g L^{-1}, the diluting solvent was NaCl, alone. Polymer–micelle complex solutions were prepared by adding prefiltered 25 g L^{-1} polymer solutions to prefiltered mixed-micelle solutions, to yield solutions with total surfactant concentrations of 14 g L^{-1} and polymer concentrations, C_P, of 0.1–0.8 g L^{-1}, in 0.40 M NaCl. For all such mixtures, the corresponding polymer-free solution was employed as the solvent for all dilutions and as the reference sample as well. Thus, the reference solvent is itself a binary mixture that contains mixed micelles and supporting electrolyte. All measurements of scattering intensity and refractive index of the complex were made relative to this medium.

For purposes of comparison, a limited number of measurements were made at Wyatt Technologies, Santa Barbara, CA, with a DAWN-B Model 16-channel photodiode array light scattering apparatus, equipped with a 5-mW linear polarized HeNe laser with beam diameter of 0.39 mm. A total of 1600 scans, corresponding to 100 scans per channel, was made for each run. To minimize the effects of dust, which were substantial, only the 10 lowest intensity scans were used. Because of the intense light source, the concentration of polymer in micellar solutions could be reduced to 0.002–0.05 g L^{-1}. As will be shown, the comparison of results obtained at the very different polymer concentrations appropriate for the two light scattering instruments provided valuable insight concerning the nature of the complex.

Refractive indexes were measured by using a Waters R401 differential refractometer. The unit was first calibrated with water in the reference cell, using sucrose solutions ranging from 0.1 to 70 wt %, corresponding to refractive index differences of 1.0×10^{-5} to 1.0×10^{-3}. Subsequently, all refractive indexes were measured relative to the diluant used for light scattering. It should be noted that dn/dc was measured with polychromatic light instead of 436-nm radiation; however, the effect of this difference in the present case is negligible.[26] dn/dc values so obtained for PDMDAAC and for Triton X-100 were in good agreement with those cited in the literature. However, reasonable dn/dc data could not be obtained for the complex; we believe this problem arises from scattering in the sample cell of the differential refractometer. Since the predominant mass of the complex is attributable to bound micelles, we assumed the dn/dc of the complex to be equal to that of the mixed micelle.

Results and Discussion

1. Light Scattering of PDMDAAC. The Zimm plot for Merquat 100 in 0.40 M NaCl is shown in Figure 1. Erratic and sometimes abrupt downward curvature was observed, irreproducibly, at scattering angle $\theta < 45°$; this was attributed to dust. However, the weak upward curvature represented by the nonlinear extrapolation in Figure 1 was reproducible and was also observed for a narrow-MWD 6×10^5 MW polystyrene standard in toluene. Furthermore, the use of quadratic fits based on data at $\theta > 45°$ to guide the extrapolations to low angle gave the correct values for $\bar{M}_w$, R_g (the radius of gyration), and A_2 (the second virial coefficient) for this polystyrene sample. The commercial PDMDAAC material employed to generate the data in Figure 1 had been characterized by

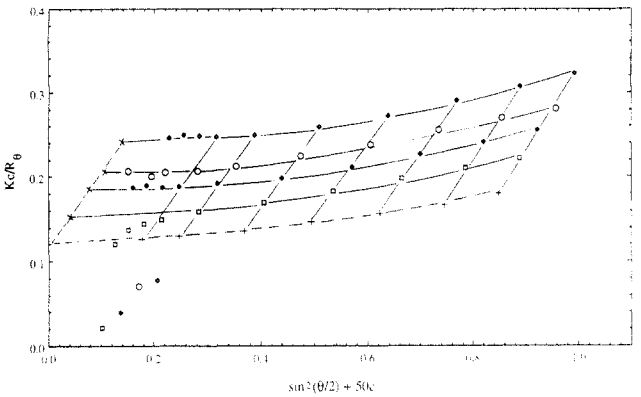

Figure 1. Zimm plot for PDMDAAC "Merquat 100" in 0.40 M NaCl. Concentrations (from upper to lower curves): (◇) 2.8 g L^{-1}, (○) 2.1 g L^{-1}, (♦) 1.4 g L^{-1}, (□) 0.7 g L^{-1}; (+) extrapolations to zero concentration, (×) extrapolations to zero angle.

the supplier, using size-exclusion chromatography, coupled with light scattering; despite the very large polydispersity, the material is reasonably well characterized, and the nominal MW of 2×10^5 is believed to be close to the weight-average MW. Table I compares our results from static light scattering and refractometry with values obtained in other work.[27] Values for R_g and A_2 are in fair agreement; values for dn/dc are identical within experimental error. The reproducibility of $\bar{M}_w$ and R_g is good. It is evident from the identity of $\bar{M}_w$ obtained in 0.40 M NaCl with the result gotten in 0.40 M NaCl + 5 mM TX-100 that there is no interaction between PDMDAAC and TX-100 micelles.

2. Light Scattering of Micelles. The Zimm plot of TX-100 (solvent: 0.40 M NaCl + 0.20 g L^{-1} TX-100) is shown in Figure 2. The plot is inverted, with a negative second virial coefficient, an observation common for micellar solutions in which there are strong intermicellar interactions.[28] Low-angle data were irreproducible and were therefore not used in extrapolation. The results for this micelle and for the mixed micelle of SDS and TX-100 ($Y = 0.35$) are shown in Table II. The appreciable growth of micelles with increase in Y and ionic strength has also been observed by QELS and size-exclusion chromatography and has been discussed elsewhere.[31]

3. Light Scattering of Polymer–Micelle Complexes. a. Selection of Conditions. Static light scattering data would be difficult to interpret if the complex structure were to change continuously with polymer concentration over the range studied. This is a well-known problem dealt with in the light scattering of associating systems.[32] While there is indeed a theoretical framework available for such systems, we wished to avoid the necessary a priori assumptions about the nature of the association process. Thus, an alternative approach is to define conditions under which variable open-ended aggregation is suppressed and the stoichiometry of the complex is invariant. A similar problem is confronted in studies of "nonstoichiometric polyelectrolyte complexes"[33] formed between "host" polyelectrolyte and "guest polyelectrolyte" of opposite charge. Kabanov and co-workers have in fact obtained "normal" Zimm plots for such equilibrium complexes.[34] While detailed experimental procedures are absent in ref 34, it appears that dissociation of intermacroionic complexes can be suppressed, particularly when the host polyelectrolyte is considerably larger than the guest, in our case PDMDAAC and the mixed micelle, respectively. It therefore seemed worthwhile to attempt to define conditions under which complex structure would remain unchanged with C_P, so that variation in polymer concentration would correspond only to variation in the number concentration of complexes, not their composition, mass, or dimensions. Such conditions might obtain if complexes remained exclusively intrapolymer, i.e. comprised of one polymer chain and a consistent number of bound micelles. This situation seemed most likely to arise at low C_P and large (excess) micelle concentrations (C_S) so that the maximum possible number of micelles would be bound, regardless of polymer concentration. One indication of this hoped-for behavior would be a linear dependence of turbidity, τ, on C_P. Therefore, solutions of mixed micelles, at a concentration of 14 g L^{-1} total surfactant, were titrated, at a constant ionic strength of 0.40 M, with Merquat 100, with the results shown in Figure 3. At low polymer concentrations, we indeed observe τ = constant × C_P. However, it is noted that a change in slope occurs in the vicinity of 0.4–0.6 g L^{-1}. Thus, the concentrations required for measurements with the Brice-Phoenix instrument sometimes exceeded those in the lowest slope region of Figure 3. The increased sensitivity of the DAWN-B, however, allowed for measurements at C_P well below 0.4 g L^{-1}.

Solutions prepared as described above were subject to QELS measurements. Our goal was to confirm that the structure of the complex was invariant with respect to C_P, using the conditions of Y, I, and C_S chosen. The QELS software discussed previously was used to generate apparent size distributions from the autocorrelation curves. The nonnegative constrained least-squares fitting algorithm used employs some added rather arbitrary compensatory procedures to avoid the selection of infinitely narrow modes when multimodal distributions are generated,[23c] so breadths of the components in the histograms seen in Figure 4 are not particularly significant. However, as we have shown before[14-16] the bimodal distributions are real, and the corresponding median apparent dimensions are meaningful. As seen in Figure 4, there is rather little change evident in the apparent average size of the complex, ca. 50 ± 15 nm for the apparent mean Stokes diameter, over the range $0.2 < C_P < 0.8$ g L^{-1}. This polymer concentration range was therefore chosen for subsequent light scattering measurements.

The definition of an "excess surfactant" solution as the diluting solvent and the restriction of polymer concentrations to relatively low values may suppress the formation of higher order aggregates, but the problem of inconstant solvent chemical potential remains. Ordinarily, light scattering of polyelectrolytes in multicomponent solvents is carried out by dilution of the polymer with solvent previously brought to dialysis equilibrium against the macroion. This approach was not feasible in the current work because the micelles do not dialyze freely but rather achieve thermodynamic equilibrium of the diffusible surfactant monomer. Free permeation of the micelle in these systems may indeed be accomplished by ultrafiltration,[16] but the requisite membrane pore size is too large to fully retain the lower MW components of Merquat 100. In the samples employed for light scattering, in which C_P is varied while the concentrations of all other components are fixed, the concentration of unbound micelles must be recognized as a variable. However, the large excess of surfactant, ranging from 20 to 1000 on a weight basis, diminishes this effect and, as we shall see, makes it possible to obtain meaningful Zimm plots.

The analysis of light scattering data requires a knowledge of the weight concentration of the solute, here defined as the polyion–micelle complex. Since the complex can-

Table I
Zimm Plot Results for PDMDAAC in 0.40 M NaCl at 24 ± 1 °C

polymer	$10^{-5}\bar{M}_w$, g mol^{-1}	R_g, nm	A_2, cm^3 mol g^{-2}	dn/dc, cm^3 g^{-1}
Merquat 100	[2.8 ± 0.8][a]	[40 ± 5][a]	[(7.3 ± 3) × 10^{-4}][a]	0.186
(nominal MW = 2 × 10^6)		[32][b]	[1.5 × 10^{-5}][b]	[0.184][b]
Merquat-100 in 5 mM TX-100 (+0.4 M NaCl)	2.0 ± 0.4	42 ± 6	(2.2 ± 1) × 10^{-3}	0.214
Cat-floc	45 ± 30	190 ± 90		[0.186][d]
(nominal MW = 2 × 10^6)	*[36 ± 10]*[c]	*90 ± 12*	*1.3 × 10^{-4}*	

[a] Average of three independent measurements (± standard deviation). [b] From ref 27. [c] Values in italics obtained with DAWN-B instrument. [d] Assumed identical to value for Merquat-100.

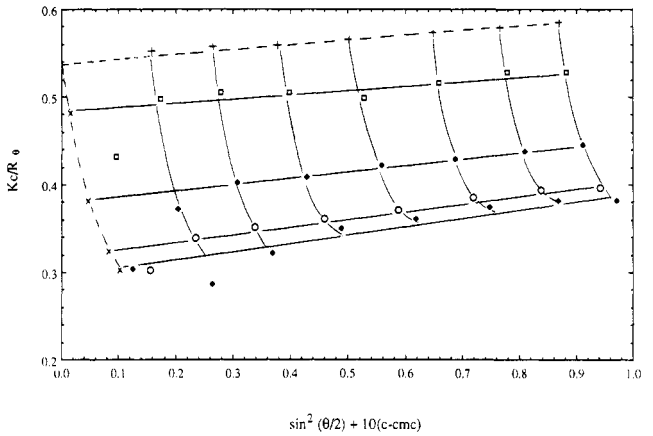

Figure 2. Zimm plot for Triton X-100 in 0.4 M NaCl + 0.20 g L^{-1} TX-100. Concentrations (from lower to upper curves): (◇) 11.8 g L^{-1}, (○) 8.8 g L^{-1}, (◆) 5.8 g L^{-1}, (□) 2.8 g L^{-1}; (+) extrapolations to zero concentration, (×) extrapolations to zero angle.

not be isolated out of solution but is instead formed in situ, its weight concentration is not a priori known. If, however, we assume a consistent stoichiometry in the complex, the ratio of the weight-average molar mass of the complex to $\bar{M}_w$ of PDMDAAC must be constant, i.e. $\bar{M}_{complex} = \beta\bar{M}_{PDMDAAC}$. The value of β may be found by the following iterative procedure. An initial value of β is assumed, and the weight concentration of the complex is calculated for every experiment by using $C_{complex} = \beta C_P$. A Zimm plot is constructed in the usual way where the abscissa is now $(\sin^2(\theta/2) + kC_{complex})$. The extrapolated value of $\bar{M}_w$ is then used to determine β, which normally differs from the arbitrary value first chosen. Typically, three such iterations were required before the value of the intercept and the complex concentrations in the Zimm plot were internally consistent. β always converged to a unique value regardless of the initial estimate.

b. Light Scattering of Complexes. A representative Zimm plot for PDMDAAC, dissolved in 14 g L^{-1} surfactant as $Y = 0.35$, in 0.4 M NaCl, is shown in Figure 5. The downward curvature observed at low angle was reproducible but was not included in the extrapolations used to obtain $\bar{M}_w$. Such curvature was substantially diminished in the much lower range of C_P accessible with the DAWN-B photogoniometer, as shown in Figure 6. Results from measurements with the two instruments are compared in Table III.

Even though the polymer concentration ranges employed for the two instruments differed by several orders of magnitude, the values of $\bar{M}_w$ for the complex formed with Merquat 100 are the same within experimental error. On the other hand, the radius of gyration obtained with the Brice-Phoenix instrument is much larger, and the Zimm plots from this instrument show reproducibly strong downward curvature at low angle. This finding is not believed to be artifactual, since the agreement between the two instruments for surfactant-free Merquat 100 was reasonably good, i.e. $\bar{M}_w = 2.0 \times 10^5$ for the Brice-Phoenix versus 3.0×10^5 for the DAWN-B instrument.

A plausible explanation for these results arises from reconsideration of Figure 3. While the data points at first glance might suggest a change in slope at $C_P \cong 0.4$, they are consistent as well with three linear regions: $0 < C_P < 0.20$, $0.20 < C_P < 0.70$, and $0.70 < C_P$. The constant slope at lower C_P which intersects the origin suggests that only intrapolymer complexes are stable below 0.2 g L^{-1} polymer, an observation in accord with numerous recent turbidimetric studies.[35] An increase in the turbidity per unit mass of added polymer at larger C_P suggest the formation of larger, i.e. multipolymer, complexes. Thus, in the concentration range employed for the measurements with the Brice-Phoenix instrument, a highly polydisperse mixture of complexes probably exist. Uncertainties in the QELS deconvolution procedure discussed above prevent us from using the data of Figure 4 in a definitive manner to describe the polydispersity of the complex. However, we tentatively note that a contribution to the scattering function corresponding to Stokes diameters in excess of ca. 100 nm arises at $C_P > 0.20$ and appears to increase with C_P. Without overinterpretation, one may certainly find evidence of higher order aggregation with increasing polymer concentration. These larger particles contribute most strongly to the scattering at low angles, hence the downward curvature of the Zimm plot of Figure 5. In the concentration range $C_P < 0.01$ shown in Figure 6, only intrapolymer complexes are formed, and very little angle dependence is observed. Similar values of $\bar{M}_w$ are obtained with the two instruments only because the evaluation of $\bar{M}_w$ from the Brice-Phoenix measurements involve, of course, extrapolation to zero polymer concentration and furthermore neglect the low-angle data where higher order aggregates contribute most strongly to the scattering. However, the low-angle data do influence the determination of R_g, so that the presence of aggregates in the higher C_P experiments is manifested in an increase in R_g.

These speculations are supported by the Guinier plots in Figure 7A, which exhibit small slope and are virtually parallel for $C_P < 0.02$ g L^{-1}. These results show that the scattering particles are relatively small and that their dimensions are independent of concentration. In contrast, Guinier plots at higher concentrations (see Figure 7B) exhibit strong curvature which increases with C_P, corresponding to a more polydisperse system whose mean dimensions increase with concentration.

It might be suggested that the high polydispersity of Merquat 100 promotes polydispersity in the complex. While the definitive studies with narrow MWD PMDAAC fractions have yet to be done, several observations are relevant. First, as seen in Table III, light-scattering data in the low concentration regime yield a radius of gyration ca. 30 nm for the complex, close to the value of ca. 35 nm for surfactant-free Merquat 100 (see Table I). Second, size-exclusion chromatography of dilute Merquat 100

Table II
Zimm Plot Results for Micelles

surfactant	solvent	$10^{-5}\bar{M}_w$	R_g, nm	A_2, cm^3 mol g^{-2}	dn/dc
TX-100	0.4 M NaCl + 0.20 g L^{-1} TX-100	0.51 ± 0.04 [0.67,[a]0.90[b]]	13 ± 4	$-(4.3 \pm 0.8) \times 10^{-4}$	0.163 [0.155][b]
SDS/TX-100 (Y = 0.35)	0.4 M NaCl	2.1 ± 0.5	21 ± 2	$-(1.4 \pm 0.8) \times 10^{-4}$	0.137

[a] From ref 29. [b] From ref 30.

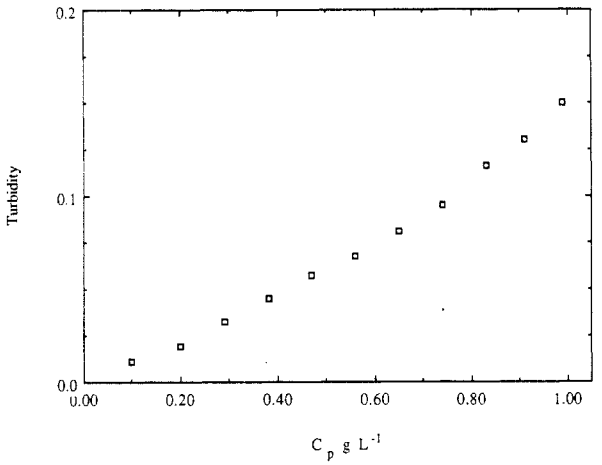

Figure 3. "Type 3" turbidimetric titration for PDMDAAC "Merquat 100" in 14 g L^{-1} mixed surfactant at Y = 0.35, in 0.4 M NaCl.

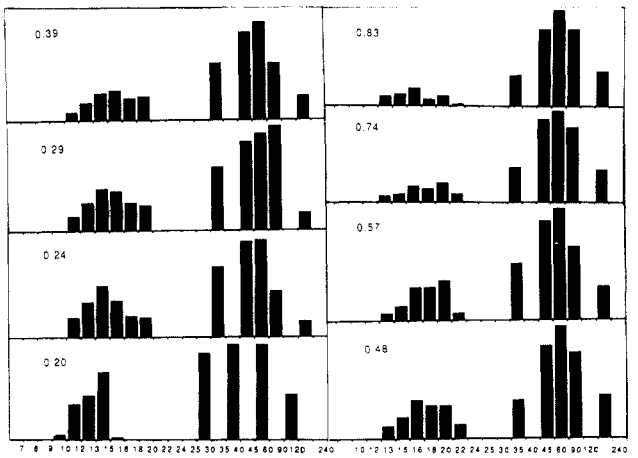

Figure 4. Distribution of apparent hydrodynamic diameters from QELS autocorrelation curves of solutions of PDMDAAC "Merquat 100" and mixed surfactant at Y = 0.35 and 14 g L^{-1}, in 0.40 M NaCl, at polymer concentrations shown (g L^{-1}). (See text for explanation.)

on a Sephadex G-200 column, with a mobile phase of 0.2 M NaCl + 40 mM TX100/10 mM SDS (Y = 0.20 is above Y_c for this ionic strength) shows a retention peak for the complex identical with that of dextran with MW = 3.5 × 10^5.[36] Last, the Guinier plots of Figures 7A do not show evidence of substantial polydispersity, in excess of that of Merquat 100. All of these findings are consistent with the formation, at low C_P, of an intrapolymer complex with dimensions and size polydispersity not much different from that of the polymer itself. (A similar result has been obtained for soluble complexes of Merquat 100 with bovine serum albumin.[37]) For C_P > 0.7 g L^{-1}, the complexes are multipolymer and presumably highly polydisperse, but the extent to which such polydispersity would be reduced with narrow MWD PDMDAAC is at present unknown.

The Zimm and Guinier plots for complex formed with high MW PDMDAAC ("Cat-floc") are shown in Figures 8 and 9, respectively. The Zimm plot is highly dis-

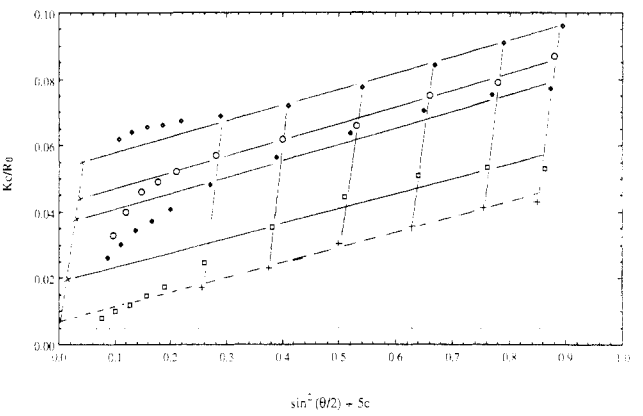

Figure 5. Zimm plot for PDMDAAC "Merquat 100" in mixed surfactant at Y = 0.35 and 14 g L^{-1}, in 0.40 M NaCl. Polymer concentrations (from upper to lower curves): (◇) 0.80 g L^{-1}, (○) 0.60 g L^{-1}, (◆) 0.40 L^{-1}, (□) 0.20 g L^{-1}; (+) extrapolations to zero concentration, (×) extrapolations to zero angle.

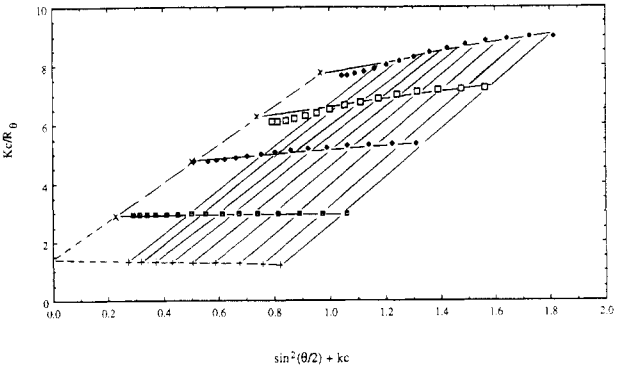

Figure 6. Zimm plot for PDMDAAC "Merquat 100" in mixed surfactant at Y = 0.35 and 14 g L^{-1}, in 0.4 M NaCl. Polymer concentrations (from upper to lower curves): (◇) 0.010 g L^{-1}, (□) 0.0075 g L^{-1}, (◆) 0.005 g L^{-1}, (⊡) 0.0025 g L^{-1}; (+) extrapolations to zero concentration, (×) extrapolations to zero angle (DAWN-B, Wyatt Technologies).

Table III
Summary of Light-Scattering Results for the PDMDAAC-SDS/TX-100 Complex[a] Formed with Micelles at Y = 0.35 in 0.40 M NaCl

PDMDAAC	$10^{-5}\bar{M}_w$, g mol^{-1}	R_g, nm	A_2, cm^3 mol g^{-2}
Merquat-100	60 ± 20	150 ± 80	5×10^{-4}
	45	*30*	*6 × 10^{-4}*
Cat-floc	*130 000*	*300*	*6 × 10^{-6}*

[a] Results in italics obtained with DAWN-B photogoniometer.

torted, even though the polymer concentrations are quite small. Comparison of Figures 9 and 7B show that linear Guinier plots are never achieved for the high MW polymer, even though that concentration range is lower. We therefore conclude that conditions in which the intrapolymer complex is the dominant form of association cannot be identified for the 2 × 10^6 MW polymer. Given the strong curvature of the Zimm plot for the Cat-floc complex, the value of the radius of gyration is highly suspect. However, neither the result for $\bar{M}_w$ nor for R_g can be explained on the basis of a 10-fold increase in MW of the polymer itself but rather suggest interpolymer com-

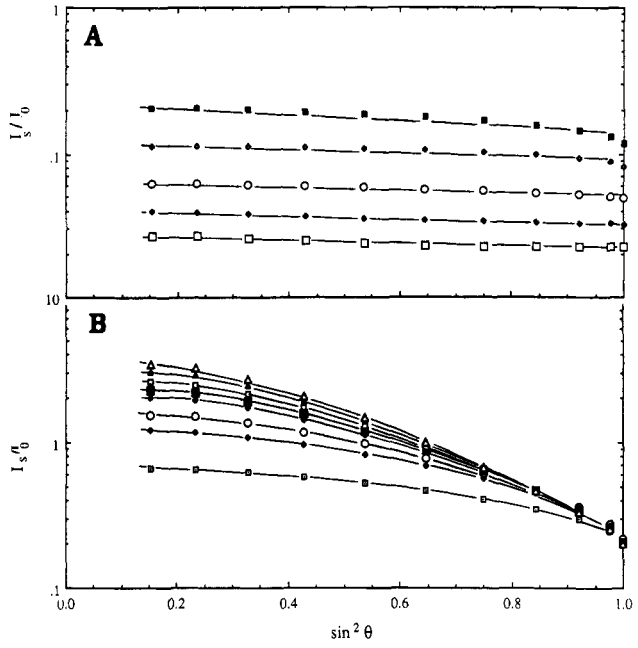

Figure 7. (A) Guinier plots, from data of Figure 6. Polymer concentrations (from lower to upper): (□) 0.0125 g L^{-1}, (♦) 0.015 g L^{-1}, (○) 0.0175 g L^{-1}, (◇) 0.020 g L^{-1}, (■) 0.0225 g L^{-1}. (B) Same as (A), but for polymer concentrations (from lower to upper): (⊡) 0.025 g L^{-1}, (♦) 0.0275 g L^{-1}, (○) 0.030 g L^{-1}, (◇) 0.0325 g L^{-1}, (■) 0.035 g L^{-1}, (□) 0.0375 g L^{-1}, (▲) 0.040 g L^{-1}, (△) 0.0425 g L^{-1}.

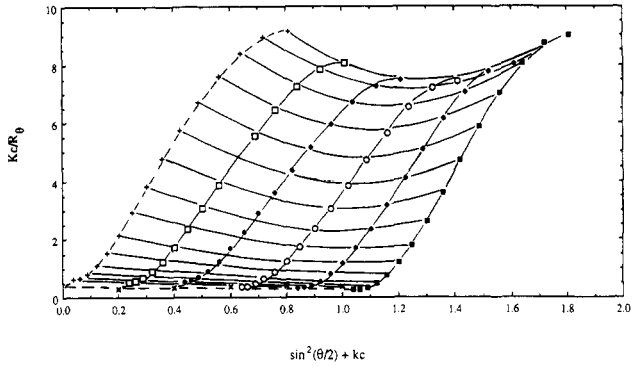

Figure 8. Zimm plot for PDMDAAC "Cat-floc" in mixed surfactant at Y = 0.35 and 14 g L^{-1}, in 0.40 M NaCl, at polymer concentrations (from right to left): (■) 0.0125 g L^{-1}, (◇) 0.010 g L^{-1}; (○) 0.0075 g L^{-1}, (♦) 0.0050 g L^{-1}, (□) 0.0025 g L^{-1}; (+) extrapolations to zero concentration, (×) extrapolations to zero angle.

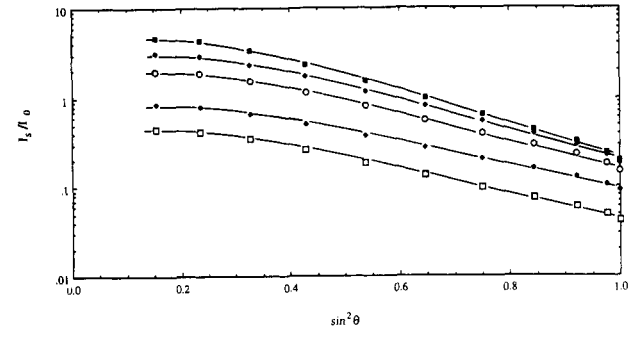

Figure 9. Guinier plots, from data of Figure 8. Polymer concentrations (from upper to lower curves): (■) 0.0125 g L^{-1}, (◇) 0.010 g L^{-1}, (○) 0.0075 g L^{-1}, (♦) 0.0050 g L^{-1}, (□) 0.0025 g L^{-1}.

plexation. The apparent order-of-magnitude increase in the radius of gyration for the Cat-floc complex versus the one formed from Merquat-100 corresponds to roughly a 1000-fold increase in the volume of the complex; this is consistent with the extraordinarily large molecular weight measured for the former.

Table IV
Comparison of Mass and Dimensions of Complex and Its Constituents

	PDMDAAC[a,b]	SDS/TX-100[b,c]	complex[a-c]
$\bar{M}_w$	(3 ● 1) × 10^5	(2 ± 0.5) × 10^5	(4.5 ± 1) × 10^6
R_g, nm	40 ± 5	21 ● 2	30

[a] Merquat 100. [b] In 0.40 M NaCl. [c] Y = 0.35.

4. Description of the Complex. Table IV reviews the values for the molar mass and the dimensions of the polymer, micelle, and complex, in 0.4 M NaCl, at Y = 0.35. The value for the radius of gyration was taken from data obtained with the DAWN-B photogoniometer only, for the following reason. The evidence formerly presented suggests that higher order aggregates can dominate the scattering at low angles for the concentrations employed in the Brice-Phoenix measurements. These low-angle data are used in determining the limiting slope, leading to the calculation of R_g. Values of R_g obtained at the higher polymer concentrations presumably represent some average dimension for a highly disperse system containing a variety of aggregates of different compositions. Therefore, it is more informative to evaluate the dimensions of the complex formed at very low polymer concentration.

The results of Table IV suggest that the complex generated at low polymer concentration is no larger than the polymer from which it is formed. This finding is in accord with previous viscometry data, which showed the reduced specific viscosity for PDMDAAC in micellar solvent to be slightly smaller than the value in 0.4 M NaCl.[11] On the other hand, the molecular weight of the complex is on the order of 10–15 times larger than the precursor polyelectrolyte. If the complex is intrapolymer, it would have to incorporate some 20 micelles, within its domain. Such a dense structure implies a considerable degree of ion pairing between PDMDAAC and the mixed micelle. In this regard, it is useful to note that polyion-micelle complexes formed (irreversibly) in pure water lose about 80–90% of the original small ions.[11]

There is at present no compelling evidence that confirms the integrity of micelle structure subsequent to binding. Therefore, as an alternative hypothesis it is necessary to consider an increase in micelle aggregation number, induced by polyion binding. The reduction of repulsion among the SDS headgroups could indeed cause micelle growth, in the same fashion as added electrolyte leads to the elongation of SDS/TX-100 mixed micelles.[31] Dye solubilization studies are underway to establish whether the solubilization efficiency of micelles is altered upon complex formation.

Acknowledgment. Support from the National Science Foundation under Grant DMR-8507479 is acknowledged.

References and Notes

(1) Robb, I. D. In *Anionic Surfactants-Physical Chemistry of Surfactant Action*; Lucassen-Reynders, E. H., Ed.; Marcel Dekker: New York, 1981; p 109.
(2) Goddard, E. D. *Colloids Surfaces* **1986**, *19*, 255, 301.
(3) Chu, D.-Y.; Thomas, J. K. *J. Am. Chem. Soc.* **1986**, *108*, 6270.
(4) Malliaris, A.; Lang, J.; Zana, R. *J. Colloid Interface Sci.* **1986**, *110*, 237.
(5) Turro, N. J.; Kuo, P.-L. *Langmuir* **1986**, *2*, 438.
(6) Abuin, E.; Lissi, E. *J. Colloid Interface Sci.* **1986**, *112*, 178.
(7) Winnik, F. M.; Winnik, M. A.; Tuzuke, S. *J. Phys. Chem.* **1987**, *91*, 594.
(8) Ruckentstein, E.; Huber, G.; Hoffman, H. *Langmuir* **1987**, *3*, 382.

(9) Cabane, B.; Duplessix, R. *J. Phys. (Les Ulis, Fr.)* **1987**, *48*, 651.
(10) Hayakawa, K.; Ohyama, T.; Maeda, T.; Satake, I.; Kwak, J. C. T. *Langmuir* **1988**, *4*, 481.
(11) Dubin, P. L.; Oteri, R. *J. Colloid Interface Sci.* **1983**, *95*, 453.
(12) Dubin, P. L.; Davis, D. D. *Macromolecules* **1984**, *17*, 1294.
(13) Dubin, P. L.; Davis, D. D. *Colloids Surfaces* **1985**, *13*, 113.
(14) Dubin, P. L.; Rigsbee, D. R.; McQuigg, D. W. *J. Colloid. Interface Sci.* **1985**, *105*, 509.
(15) Dubin, P. L.; McQuigg, D. W.; Rigsbee, D. R. *Polym. Prep. (Am. Chem. Soc. Div. Polym. Chem.)* **1986**, *27* (1), 420.
(16) Dubin, P. L.; Rigsbee, D. R.; Fallon, M. A.; Gan, L. M. *Macromolecules* **1988**, *21*, 2555.
(17) Dubin, P. L.; Thé, S. S.; McQuigg, D. W.; Gan, L. M.; Chew, C. H. *Langmuir* **1989**, *5*, 89.
(18) Dubin, P. L.; Gan, L. M.; Chew, C. H. *J. Colloid Interface Sci.* **1989**, *128*, 566.
(19) Dubin, P. L.; Skelton, J.; Curran, M., Sudbeck, E., in preparation.
(20) Koppel, D. E. *J. Chem. Phys.* **1972**, *57*, 4814.
(21) Strege, M. A.; Dubin, P. L. *J. Chromatogr.* **1989**, *463*, 165.
(22) Lin, F. M. Calgon Corp., private communication.
(23) (a) Provencher, S.; Hendrix, J.; de Maeyer, L. *J. Phys. Chem.* **1978**, *69*, 4273. (b) Provencher, S. *Makromol. Chem.* **1979**, *180*, 20. (c) Nicoli, D. F. Private communication.
(24) Morrison, I. D.; Grabowski, E. F.; Herb, C. A. *Langmuir* **1985**, *1*, 496.
(25) In the Nicomp software, "fit error" is obtained from the sum of the squares of the errors between the fitted autocorrelation curve and the measured one, normalized with respect to particle size, while the "residual" is the coefficient obtained for the decay constant corresponding to an infinitely large particle, and is frequently attributed to dust "events".
(26) Huglin, M. B. In *Light Scattering from Polymer Solutions*; Huglin, M. B., Ed.; Academic Press: New York, 1972; p 165.
(27) Burkhardt, C. W.; McCarthy, K. J.; Parazak, D. P. *J. Polym. Sci., Polym. Lett. Ed.* **1987**, 25, 209.
(28) Imae, T.; Ikeda, S. *Colloid Polym. Sci.* **1984**, *262*, 497.
(29) Mankowich, A. M. *J. Phys. Chem.* **1954**, *58*, 1027.
(30) Kushner, L. M.; Hubbard, W. D. *J. Phys. Chem.* **1954**, *58*, 1163.
(31) Dubin, P. L.; Principi, J. M.; Smith, B. A.; Fallon, M. A. *J. Colloid Interface Sci.* **1989**, *127*, 558.
(32) See, for example: Elias, H.-G. in ref 26, Chapter 9.
(33) For reviews, see: (a) Tsuchida, E.; Abe, K. In *Interactions between Macromolecules in Solution and Intermacromolecular Complexes*; Advances in Polymer Science 45; Springer-Verlag: Berlin, 1982. (b) Smid, J.; Fish, D. In *"Encyclopedia of Polymer Science and Technology*; Wiley-Interscience: New York, 1988, Vol. 11, p 720.
(34) (a) Kharenko, O. A.; Kharenko, A. V.; Kasaikin, V. A.; Zezin, A. B.; Kabanov, V. A. *Polym. Sci. USSR (Engl. Transl.)* **1980**, *21*, 3009 (translation of *Vysokomol. Soyed.* **1979**, *A21*, 2726). (b) Kabanov, V. A.; Zezin, A. B. *Makromol. Suppl.* **1984**, *6*, 259.
(35) Dubin, P. L.; Vea, E. M. Y.; Thé, S. S. *Abstracts*, Colloid and Surface Science Division; National Meeting of the American Chemical Society, Miami Beach, FL, Sept 1989; *Langmuir*, in press.
(36) Fallon, M. A. Thesis, Purdue University, 1986.
(37) (a) Dubin, P. L.; Murrell, J. M. *Macromolecules* **1988**, *21*, 2291. (b) Strege, M. A.; Dubin, P. L.; Flinta, C. D.; West, J. S. In *Downstream Processing and Bioseparation*; Hamel, J.-F. P., Hunter, J. B., Sikdar, S. K., Eds.; ACS Symposium Series 419; American Chemical Society: Washington, DC, 1990; p 158.

Flow and Viscoelastic Properties of Xanthan Gum Solutions

Michel Milas and Marguerite Rinaudo*

Centre de Recherches sur les Macromolécules Végétales, CNRS, BP 53 X, 38041 Grenoble Cedex, France

Magali Knipper and Jean Luc Schuppiser

Rhône Poulenc, Centre de Recherches d'Aubervilliers, 52, Rue de la Haie Coq, 93308 Aubervilliers Cedex, France. *Received May 16, 1989; Revised Manuscript Received October 31, 1989*

ABSTRACT: This paper concerns the rheological behavior of an unpasteurized sample of xanthan as a function of the polymer concentration and of the conformation of the polysaccharide. The evidence of critical concentrations (C^* and C^{**}) is discussed from steady shear and dynamic experiments. The behavior of the xanthan solutions is characteristic of polymeric solutions without any evidence of gellike character in contrast with the results obtained previously on commercial samples.

Introduction

Xanthan is a bacterial polysaccharide which has been widely studied in recent years. However, the results diverge on many aspects such as the nature of the ordered structures[1] or the influence of the substituents on its properties in solution.[2] In contrast, an apparent agreement exists about the conformational transition in solution and its dependence with temperature, ionic strength, and substituent contents. In fact, only a few studies take into account the existence of two different ordered conformations in solution (native and renatured) which modify the hydrodynamic and rheological properties but not the position of the conformational transition;[3] aggregates which are generally present in commercial xanthan samples lead to the same behavior.

Concerning the conformation of xanthan in solution, the chain model usually adopted now is that of a wormlike chain characterized by an intrinsic persistence length either around 500 Å if we adopt the single helix as ordered conformation[4] or around 1200 Å in the case of a double helix.[5]

A first approach of the viscoelastic properties of xanthan gum was made by Thurston et al. in 1981.[6] These authors showed that the same relaxation processes are responsible for both the steady and the oscillatory flow behavior and were sufficient to describe how the viscoelasticity changes with both shear rate and frequency and how the steady flow viscosity changes with shear rate.

0024-9297/90/2223-2506$02.50/0